ELSEVIER

Contents lists available at ScienceDirect

# Deep-Sea Research Part II

journal homepage: www.elsevier.com/locate/dsr2



# An N isotopic mass balance of the Eastern Tropical North Pacific oxygen deficient zone



Clara A. Fuchsman<sup>a,\*</sup>, Allan H. Devol<sup>a</sup>, Karen L. Casciotti<sup>b</sup>, Carolyn Buchwald<sup>c,d</sup>, Bonnie X. Chang<sup>a,e,f</sup>, Rachel E.A. Horak<sup>a</sup>

- <sup>a</sup> University of Washington, School of Oceanography, Seattle, WA, United States
- <sup>b</sup> Stanford University, Stanford, CA, United States
- <sup>c</sup> Massachusetts Institute of Technology/Woods Hole Oceanographic Institution Joint Program in Chemical Oceanography, Woods Hole Oceanographic Institution, Woods Hole, MA, United States
- <sup>d</sup> Dalhousie University, Halifax, Nova Scotia, Canada
- <sup>e</sup> National Oceanic and Atmospheric Administration, Pacific Marine Environmental Lab, Seattle, WA, United States
- <sup>f</sup> JISAO (Joint Institute for the Study of the Atmosphere and Ocean), Seattle, WA, United States

#### ARTICLE INFO

# Keywords: Nitrogen isotopes Oxygen deficient zone Nitrogen gas Eastern Tropical North Pacific

#### ABSTRACT

Oxygen deficient zones host up to 50% of marine  $N_2$  production and the Eastern Tropical North Pacific (ETNP) is the largest marine oxygen deficient zone. We measured  $\delta^{15}N\text{-NO}_3$ ,  $\delta^{15}N\text{-NO}_2$ , and  $\delta^{15}N\text{-N}_2$  at 7 stations along a transect normal to the coast in the heart of the ETNP oxygen deficient zone in 2012. The  $\delta^{15}N\text{-N}_2$  minimum was 0.34% at 300 m, which corresponded with the  $N_2$ :Ar maximum. When the atmospheric  $N_2$  background was removed, the biological  $\delta^{15}N\text{-NO}_2$  for the ODZ ranged from -7% to -22%. In the ODZ,  $\delta^{15}N\text{-NO}_3$  ranged from 15 to 24% while  $\delta^{15}N\text{-NO}_2$  was generally between -11 and -18%, generating differences up to 40% between  $\delta^{15}N\text{-NO}_3$  and  $\delta^{15}N\text{-NO}_2$ . The isotopic separation between nitrite and nitrogen gas ( $\Delta^{15}N_{NO2-N2}$ ) changed sign from  $\sim 5\%$  at the top of the oxygen deficient zone to  $\sim -10\%$  at 300 m, indicating an important shift in nitrogen cycling with depth. We calculated the closed system Rayleigh isotope effect ( $\epsilon$ ) for  $N_2$  production from both the  $\delta^{15}N\text{-DIN}$  ( $\epsilon_{\text{DIN}}=26\pm11\%$ ) and  $\delta^{15}N\text{-N}_2$  ( $\epsilon_{N2}=27\pm6\%$ ) data. When examined individually by depth, both  $\epsilon_{\text{DIN}}$  and  $\epsilon_{N2}$  matched closely and both  $\epsilon$  depth profiles showed maximal fractionation at 300 m. Additionally, closed system isotope effects were calculated for one offshore station from the Arabian Sea in 2007 using  $\delta^{15}N\text{-N}_2$  ( $\epsilon_{N2}=24\pm4\%$ ) and  $\delta^{15}N\text{-DIN}$  ( $\epsilon_{\text{DIN}}=26\pm3\%$ ). The relatively large isotope effects for  $N_2$  production appear to be found in both major offshore oxygen deficient zones, which implies a large denitrification term in the marine N budget.

### 1. Introduction

Fixed nitrogen, e.g. nitrate, nitrite and ammonia, is essential for the growth of phytoplankton and other microbes, and limits primary production in much of the surface ocean (Moore et al., 2013). The balance between  $N_2$  fixation and  $N_2$  production controls the amount of marine fixed-N present in the ocean (Brandes and Devol, 2002; DeVries et al., 2012). There are three major oxygen deficient zones (ODZs) in the ocean: the Arabian Sea in the Indian Ocean, the Eastern Tropical North Pacific (ETNP) and the Eastern Tropical South Pacific (ETSP). Despite constituting < 1% of the ocean volume, ODZs host 30–50% of marine fixed-N loss through  $N_2$  production (DeVries et al., 2013). Evidence suggests that the oxygen content of the Pacific is decreasing (Ito et al., 2017, 2016; Stramma et al., 2008; Whitney et al., 2007) and a 1%

reduction in the ocean  $O_2$  inventory could double the size of ODZs (Deutsch et al., 2011). Indeed, repeat measurements along  $110^\circ$  W longitude in the eastern tropical North Pacific (ETNP) indicate that the ODZ thickness has increased over the past 40 years (Horak et al., 2016). The oxygen content of the ocean is sensitive both to temperature, and to increases in anthropogenic iron deposition (Ito et al., 2016). While the current decrease in oxygen is likely due to anthropogenic impacts and the Pacific Decadal Oscillation, the volume of ODZs should also increase with future climate change (Ito et al., 2016; Ito and Deutsch, 2013). Thus, ODZs are predicted to expand in the future, increasing the area favorable for fixed-N loss.

Although we have a reasonably good idea of the magnitude of fixed-N loss through denitrification (org C + NO<sub>3</sub>-  $\rightarrow$  N<sub>2</sub>) and anammox (NH<sub>4</sub><sup>+</sup> + NO<sub>2</sub><sup>-</sup>  $\rightarrow$  N<sub>2</sub>) in the three major ODZs (Chang et al., 2012,

E-mail address: cfuchsm1@u.washington.edu (C.A. Fuchsman).

<sup>\*</sup> Corresponding author.

2010), our understanding of the factors affecting these two processes is still limited. The interpretation of the stable isotopic composition of the reactants and products of the N-cycle provides a way to examine low oxygen systems without manipulation or incubation. To date there are relatively few studies examining the δ<sup>15</sup>N-N<sub>2</sub> in low oxygen waters (Altabet et al., 2012; Bourbonnais et al., 2015; Brandes et al., 1998; Cline and Kaplan, 1975; Fuchsman et al., 2008; Hu et al., 2016; Manning et al., 2010). Older studies such as Brandes et al. (1998) and Cline and Kaplan (1975) examine  $\delta^{15}$ N-N<sub>2</sub> in offshore oxygen deficient waters but the authors did not use  $\delta^{15}$ N-N<sub>2</sub> to calculate isotope effects. Many of the recent  $\delta^{15}$ N-N<sub>2</sub> measurements have been on the Peru shelf of the ETSP and the region offshore of the shelf which is affected by upwelling and eddies (Altabet et al., 2012; Bourbonnais et al., 2015; Hu et al., 2016). In this system, nitrate concentrations are low and can be drawn down to zero. This differs from far offshore ODZs where nitrate concentrations are consistently between 20 and 30 µM (Chang et al., 2012, 2010). It was found that the isotope effect for N<sub>2</sub> production from nitrate was small, as low as 11% on the Peru shelf (Hu et al., 2016) and 14‰ in a eddy off shore of the shelf (Bourbonnais et al., 2015). While no studies in the ETNP and Arabian Seas have previously examined the isotope effect for N<sub>2</sub> production from the N<sub>2</sub> perspective, studies on the isotopic composition of dissolved inorganic N ( $\delta^{15}$ N-DIN) in offshore oxygen minimum zones in the 1990s has yielded closed isotope effect estimates of  $\varepsilon_{DIN} = 22-25\%$  (Brandes et al., 1998; Voss et al., 2001). The  $\delta^{15}$ N-DIN data from the ETNP in 1972 yielded open system isotope effect estimates of 30% to 40% (Cline and Kaplan, 1975), but the  $\delta^{15}$ N-DIN values were actually similar to those seen in the 1990s. Thus, current estimates for the N2 production isotope effect vary from 11% to 40‰.

Studies of cultured bacteria also yield large range of estimates for isotope effects involved in steps of N2 production. Wastewater anammox bacteria have a nitrite reduction isotope effect of  $\varepsilon_{NO2}$  =  $16 \pm 4\%$  (Brunner et al., 2013). Denitrifier cultures grown at slow growth rates and reduced C source produced small isotope effects for nitrate reduction ( $\varepsilon_{NO3}=10$  to 15%; Kritee et al., 2012). However, denitrifier cultures grown at fast growth rates had large isotope effects ( $\varepsilon_{NO3}$  up to 30%; (Granger et al., 2008; Kritee et al., 2012). The nitrate reduction isotope effect should not be confused with the isotope effect for N2 production (Fig. 1). While Bourbonnais et al. (2015) found an isotope effect for N2 production of 14% in an ETSP eddy, they also found an isotope effect for nitrate reduction of 16-21‰. Similarly, a recent modeling study of  $\delta^{15}N-NO_2$  and  $\delta^{15}N-NO_3$  in the ETSP found that an isotope effect of 18-23% for nitrate reduction best fit the available data (Peters et al., 2016). This difference between the isotope effect of N<sub>2</sub> production and nitrate reduction highlights the importance of looking at actual  $\delta^{15}$ N-N<sub>2</sub> data.

In the marine environment, the apparent isotope effect between nitrate and  $N_2$  is affected by nitrite oxidation (Fig. 1). Nitrite oxidation has an inverse isotope effect, making nitrite more depleted and nitrate more enriched (Casciotti, 2009). The difference between  $\delta^{15}N\text{-NO}_3$  and  $\delta^{15}N\text{-NO}_2$  ( $\Delta^{15}N$ ) can reach 40 to 50‰ in low oxygen waters (Bourbonnais et al., 2015; Buchwald et al., 2015; Gaye et al., 2013; Hu et al., 2016; Martin and Casciotti, 2017). Although it has been suggested that ODZs are functionally anoxic (Revsbech et al., 2009; Ulloa et al., 2012), the low oxygen  $K_m$  for nitrite oxidation  $0.5 \pm 4\,\text{nM}$  (Bristow et al., 2016), indicates nitrite oxidation is possible at oxygen concentrations below detection of a STOX oxygen sensor (1–10 nM; Ulloa et al., 2012). Furthermore, rates of oxygen advection and

$$\begin{array}{c} \textit{nitrate red. nitrite red.} \\ \text{NO}_{3} \xrightarrow[\epsilon_{ox}]{\epsilon_{NO2}} \text{NO}_{2} \xrightarrow[\epsilon_{ox}]{\epsilon_{NO2}} \text{N}_{2} \\ \textit{nitrite ox.} & \text{NH}_{4}^{+} \text{ completely consumed)} \end{array}$$

Fig. 1. Schematic depicting individual isotope effects and N sources that are included in the apparent isotope effect for  $N_2$  production.

diffusion may be large enough to supply the necessary oxygen to the upper and lower parts of the ODZ, but not the core (Peters et al., 2016). Stable  $\delta^{15}N$  and  $\delta^{18}O$  isotopes indicate parallel processes of nitrite oxidation and dentrification in ODZs (Buchwald et al., 2015; Gaye et al., 2013; Martin and Casciotti, 2017; Peters et al., 2016). In large ODZs, measured and modeled nitrite oxidation rates dwindle in the core of the ODZ, but the depth range of nitrite oxidation and  $N_2$  production overlap (Babbin et al., 2017, 2014; Buchwald et al., 2015; Peng et al., 2015; Penn et al., 2016; Peters et al., 2016).  $\delta^{15}N$ -NO $_3$  and  $\delta^{15}N$ -NO $_2$  are affected oppositely by nitrite oxidation, but their combined isotopic pool (DIN) is unaffected. However many  $N_2$  production processes use nitrite directly, so changes in  $\delta^{15}N$ -NO $_2$  from nitrite oxidation would affect their  $N_2$  isotopic signature.

Unlike water column denitrification, sedimentary denitrification is thought to usually have a very small isotope effect (< 3%) due to near complete consumption of nitrate (Brandes and Devol, 1997; Lehmann et al., 2007; Sigman et al., 2003). Higher fractionation effects have been documented (Dähnke and Thamdrup, 2013), but in general the isotope effect is thought to be small. The balance between sedimentary denitrification and water column denitrification sets the  $\delta^{15}N$  of oceanic DIN. Thus, the isotope effect from nitrate to N2 during water column denitrification can be used to estimate rates of sedimentary denitrification. A large isotope effect associated with denitrification in offshore ODZs implies significantly more sedimentary denitrification than water column denitrification (Brandes and Devol, 2002). A small fractionation effect for water column denitrification reduces estimates of sedimentary denitrification and requires less N2 fixation to attain global marine N balance (Altabet, 2007; Bourbonnais et al., 2015; Brandes and Devol, 2002; Kritee et al., 2012). DeVries et al. (2013) were able to model the a balanced ocean N budget with a 3-D biogeochemical model using an apparent isotope effect for nitrate reduction of 17% and a marine denitrification rate of 120–240 Tg N yr<sup>-1</sup> (DeVries et al., 2013). However, an isotope effect significantly larger than 17% could potentially imply both larger sources and sinks of N<sub>2</sub> in the ocean.

The Eastern Tropical North Pacific (ETNP) ODZ is the largest Oxygen Minimum Zone (Paulmier and Ruiz-Pino, 2009) with over 700 m depth of anoxic water at its heart. Here we present  $\delta^{15}\text{N-N}_2$ ,  $\delta^{15}\text{N-NO}_2$ , and  $\delta^{15}\text{N-NO}_3$  from 7 stations in the heart of the ETNP ODZ including both coastal and far offshore stations (Fig. 2; Table S1). Additionally we examine data from one station in the Arabian Sea (Table S1) to expand the range of our findings. Here we present the first analysis of the denitrification isotopic effect based on  $\delta^{15}\text{N-N}_2$  outside of the ETSP.

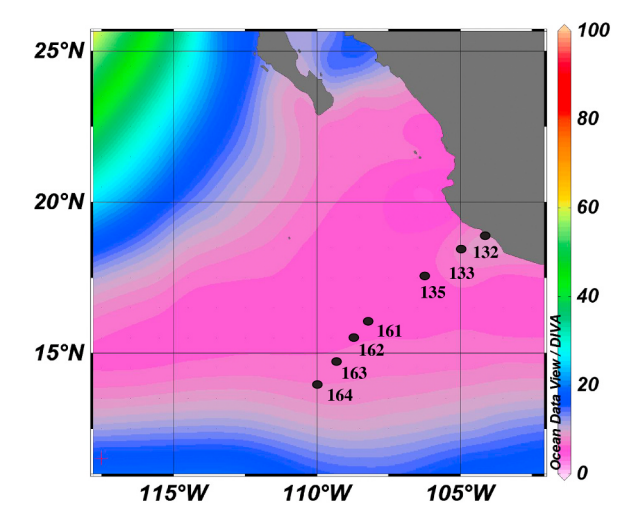


Fig. 2. A map of the Eastern Tropical North Pacific shaded by oxygen concentration according to the World Ocean Atlas (2013) (Garcia et al., 2013) at density surface  $\sigma=26.5$ . Black dots indicate stations examined in this paper.

#### 2. Methods

#### 2.1. Study site and sample collection

Samples were collected during R/V Thomas G. Thompson cruise TN278 to the ETNP during March-April 2012 (Fig. 2, Table S1). Water samples were taken using a SeaBird CTD-Rosette system equipped with dual sensors for conductivity, temperature, and oxygen (SBE 043) as well as Chlorophyll fluorescence and transmissivity. A STOX (Switchable Trace Oxygen microsensor; Revsbech et al., 2009) sensor was also attached to the CTD-Rosette and its output was also logged by the CTD. (The STOX data from this cruise has been previously reported in Tiano et al., 2014). The SeaBird SBE43 oxygen sensor was calibrated against Winkler determinations (n = 53 depths in triplicate, regression  $R^2 = 0.98$ ).

Samples were also collected on the R/V Roger Revelle at Station 1 (Table S1) in the Arabian Sea during September 2007. Water samples were taken using a SeaBird CTD-Rosette system equipped with dual sensors for conductivity, temperature, and oxygen (SBE 043). The SeaBird SBE43 oxygen sensor was calibrated against micro-Winkler determinations.

#### 2.2. Nutrient measurements

For the ETNP, nutrient samples collected directly from the Niskin bottles and were filtered through GF/F glass fiber filters and stored refrigerated until analysis on board. Concentrations of  $\mathrm{NO_2}^-$ ,  $\mathrm{PO_4}^{3-}$ , Si (OH)<sub>4</sub>, and  $\mathrm{NH_4}^+$  were determined shortly after sample collection using a Technicon Autoanalyzer and the JGOFS protocols (UNESCO, 1994). For the Arabian Sea, nutrient values were reported in Chang et al. (2012).

#### 2.3. $N_2$ and $\delta^{15}N-N_2$ methods

For the ETNP, duplicate gas samples used for  $N_2$ :Ar ratios and  $\delta^{15}N_2$  were collected in preweighed, evacuated 185 mL glass flasks sealed with a Louwers-Hapert valve. The sampling flask contained dried mercuric chloride as a preservative (Emerson et al., 1999). To prevent air contamination when sampling, samples were transferred from the Niskin bottle to the sample flask under a local  $CO_2$  atmosphere (Emerson et al., 1999). Sample flasks were filled approximately half full and returned to the University of Washington for analysis. In the laboratory flasks were weighed and equilibrated with the headspace by rotating overnight in a water bath at a known (room) temperature. Immediately after equilibration nearly all liquid water was removed from the flask and the head-space gases were cryogenically processed to completely remove  $CO_2$  and residual water vapor. At the same time a known concentration of  $^{36}Ar$  spike was added to each sample, as done previously (Chang et al., 2010; Fuchsman et al., 2008), to allow the concentration of  $^{40}Ar$  to be determined from the  $^{36}Ar$ : $^{40}Ar$  ratios.

To avoid using an oxygen correction for  $\delta^{15}$ N-N<sub>2</sub>, most oxic samples were also put through an inline CuO furnace to remove all oxygen. However, to check the validity of the oxygen correction, for some duplicates, one sample was put through the furnace and one was not. The still oxygenated samples were measured against an oxygenated standard and an oxygen correction was used as in (Chang et al., 2012, 2010; Fuchsman et al., 2008; Manning et al., 2010). Duplicates matched indicating that present and older data were comparable (Fig. S1). All gas samples were measured at the Stable Isotope Lab, School of Oceanography, University of Washington on a Finnigan Delta XL isotope ratio mass spectrometer. Anoxic samples were measured against a standard containing zero oxygen, where the standard value was determined from air heated in the inline CuO furnace to remove oxygen.

Also included here are  $\delta^{15}$ N-N<sub>2</sub> measurements from the Arabian Sea in 2007. N<sub>2</sub> concentrations for these samples have been previously reported (Chang et al., 2012). However,  $\delta^{15}$ N-N<sub>2</sub> values have not been

previously reported. They were measured as above except that a CuO furnace was not used. The effect of oxygen on the measurement of  $\delta^{15} N$  was determined using a series of five flasks that contain variable amounts of oxygen but the same concentrations and  $\delta^{15} N$  of nitrogen gas. The calculated slope from the standards was extrapolated to the sample. The value of the oxygen correction ranged from zero in the ODZ to 0.1–0.3% in oxic waters.

In the Black Sea, a methane correction was used for  $\delta^{15} N \cdot N_2$  (Fuchsman et al., 2008), but in the Black Sea methane can reach 11  $\mu$ M (Reeburgh et al., 1991). This correction was not needed in the ETNP or Arabian Sea because methane was  $\leq 100 \, \text{nM}$  in these ODZs (Chronopoulou et al., 2017; Javakumar et al., 2001).

# 2.4. $\delta^{15}$ N-NO<sub>2</sub>, and $\delta^{15}$ N-NO<sub>3</sub> methods

Samples containing  $[NO_2] > 0.25 \,\mu\text{M}$  were chosen for  $\delta^{15} \text{N-NO}_2$ analysis, purged with N2 gas to remove in situ N2O, and treated with a sodium azide/acetic acid reagent (McIlvin and Altabet, 2005). Nitrite isotope analyses were conducted on 2-10 nmol of NO<sub>2</sub> and calibrated to air and VSMOW reference scales (for  $\delta^{15}$ N and  $\delta^{18}$ O, respectively) using reference materials N-23, N-7373, and N-10219 (Casciotti et al., 2007) each analyzed in triplicate at two different quantities (5 nmol and 10 nmol  $NO_2$ ).  $\delta^{15}N-NO_3$  samples were prefiltered with 0.2  $\mu m$ syringe filters and frozen until returning to the lab. Sulfamic acid was added to samples containing  $[NO_2^-] > 0.2 \,\mu\text{M}$  to remove  $NO_2^-$  (Granger and Sigman, 2009). δ<sup>15</sup>N-NO<sub>3</sub> was determined by the 'denitrifier method', which involves the bacterial conversion of NO<sub>3</sub><sup>-</sup> to N<sub>2</sub>O (Casciotti et al., 2002; Sigman et al., 2001). Nitrate isotope analyses were conducted on 20 nmol NO3- and calibrated to air and VSMOW reference scales (for  $\delta^{15}N$  and  $\delta^{18}O$ , respectively) using reference materials USGS32, USGS34, and USGS35 (Bohlke et al., 2003), each analyzed six times throughout the run in 20 nmol amounts (McIlvin and Casciotti, 2011).  $\delta^{15}$ N-NO<sub>2</sub>, and  $\delta^{15}$ N-NO<sub>3</sub> from station 1 in the Arabian Sea 2007 were measured similarly and can be seen in Martin and Casciotti (2017).

# 3. Results

The section comprised by our stations in the ETNP showed a significant upward tilt of the isopleths surfaces near the coast (Fig. 3). At stations 132 and 133, the stations closest to the coast (Fig. 2), the top of the ODZ and the nitrite maximum were at shallower depths than open ocean stations on the transect (Fig. 3). Due to this, we present the offshore stations data versus depth, but when all stations are combined we plot versus density. At the offshore stations (Fig. 2) the STOX based  $O_2$  concentrations became undetectable at 105 m and remained undetectable until 830 m (Tiano et al., 2014). We define the ODZ as this zone over which oxygen was below detection.

The top of the ODZ was also the depth at which a secondary nitrite maximum (SNM) appeared in the water column (Fig. 4a). At the offshore stations, the concentration of NO<sub>2</sub> in the SNM increased to  $\sim$  5  $\mu M$  at 140 m and then decreased to zero at 500 m (Fig. 4a), while at the coastal stations the maximum was greater ( $\sim$  6  $\mu M$ ) and occurred shallower in the water column (Fig. 3 and S2). Nitrate concentrations were very low in the mixed layer, increased rapidly in the pycnocline to about 20  $\mu M$ , then increased more gradually to a maximum of about 45  $\mu M$  at 1000 m (Fig. 4a). Ammonium concentrations were generally < 0.1  $\mu M$  in the ODZ (Peng et al., 2015; Fig. S3), so we consider DIN to be NO<sub>3</sub> + NO<sub>2</sub>. DIN concentrations were similar to nitrate with the exception of a significant elevation in the upper half of the ODZ due to the secondary nitrite maximum.

Data from all stations, coastal and offshore, aligned well on density surfaces (Fig. S4). At all stations, the SNM peak was located on the 26.2 sigma-theta surface. This sigma-theta surface coincides with the Pacific Equatorial  $13\,^{\circ}\text{C}$  water mass (Fig. S5) discussed in (Fiedler and Talley, 2006).

400

600

800

200

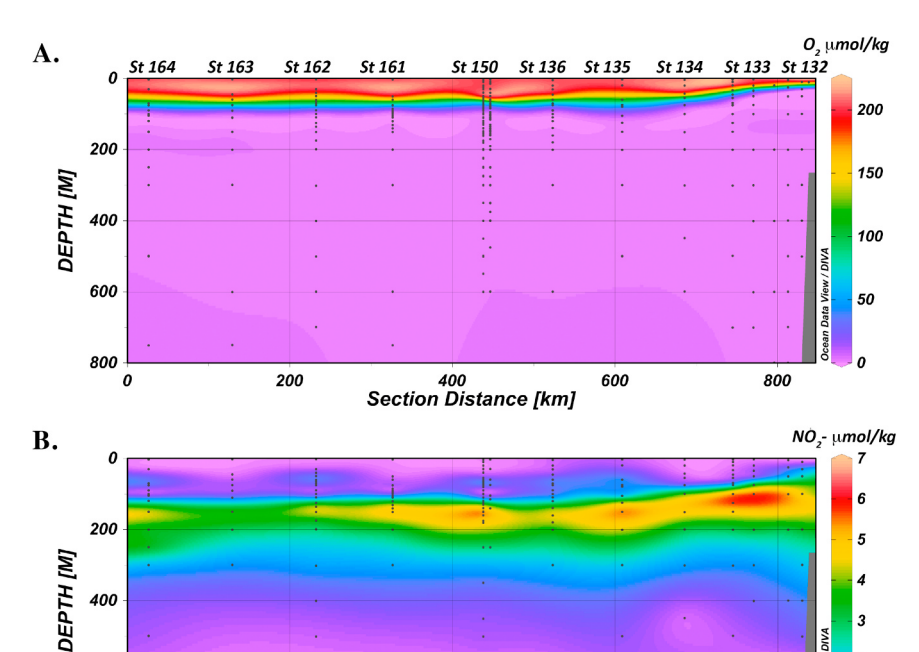
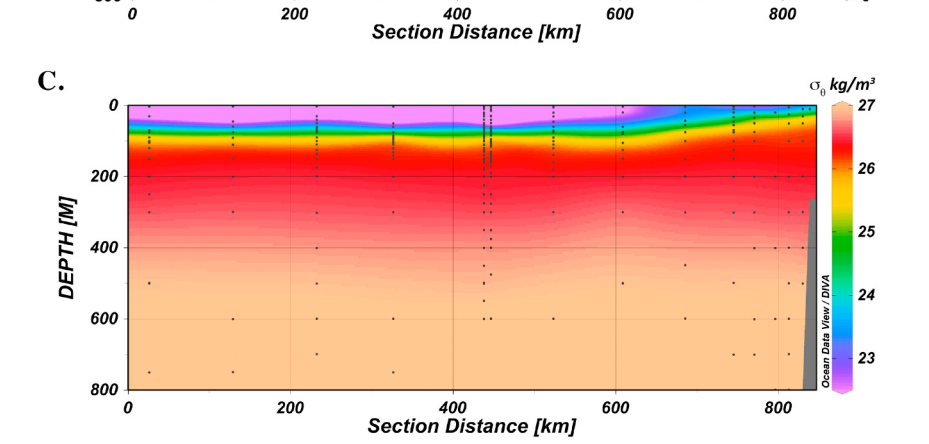


Fig. 3. Section plot of A) oxygen (umol/kg), B) nitrite (umol/kg) and C) potential density (kg/m3) for the ETNP in 2012. Sampled depths are indicated by black dots. Station names are listed at the top of part A and include some stations where isotope data was not available. The shelf is indicated by dark grey.



# 3.1. Nitrogen gas and $\delta^{15}N$

Measured N2:Ar saturation ratios were high in the ODZ and frequently had two local maxima, one at the top of the ODZ and a second at 300 m (Fig. S2). Measured N2:Ar ratios contain both biologically produced N2 and a large background signal. The background N2 (and argon) was originally derived from equilibrium with air, but mixing of water masses of different temperatures causes gases to become supersaturated in the ocean (Ito and Deutsch, 2006). We determined biological N2 (N2 excess) by subtracting background N2:Ar measurements from oxic waters in the tropical and subtropical Pacific (Chang et al., 2012). The background data was fit with the equation:

$$N_2: Ar_{Background} = 0.998 + 2.31 \times 10^{-8} e^{0.49\sigma_{\theta}}.$$
 (1)

Calculated background values for each station are shown in Fig. S2. N<sub>2</sub> excess, which we consider to be biological N<sub>2</sub>, was then calculated as follows:

$$N_{2,excess} = (N_2 : Ar_{measured} - N_2 : Ar_{Background}) \times N_{2,saturation} \times 2$$
 (2)

Where the factor of 2 in the last term converts from moles of N2 gas to moles N.

N<sub>2,saturation</sub> was calculated as in Hamme and Emerson (2004). Thus Ar measurements were not used in the calculation of N2 excess reported

here. Argon concentrations were up to 6% supersaturated in the upper oxic waters, but were very close to saturation in the ODZ (Fig S6). Since the argon measurements were close to saturation, using Ar measurements to determine N2 concentrations from N2:Ar measurements and background calculations, instead of  $N_{2,saturation}$ , produced quite similar results (Fig. S7). N2 excess values were high through the ODZ with concentrations between 10 and 15 µM (Fig. 4 and S2).

The amount of fixed N loss in an ODZ, has frequently been expressed as N deficit, which is the difference between measured [DIN] and expected DIN. The expected DIN (Nexpected) is typically estimated from phosphate to DIN ratios determined from waters outside the ODZ and phosphate concentrations within the ODZ:

$$N_{\text{expected},ETNP} = 14.4 \times [PO_4^{3-}] - 1.1.$$
 (3)

In the ETNP, depth distribution of N deficit generally matches N2 excess (Fig. 4), with N deficit, like N2 excess, maximal at the top of the ODZ and at 300 m. There is a local minimum in both N deficit and N2 excess located at 200 m (density surface 26.3). In general, N2 excess and N deficit values match closely with a slope of 0.9 ( $R^2 = 0.86$ ; Fig. S8). However, at stations 162 and 163 there is a significant mismatch (2-4 µM) between N deficit and N2 excess in the ODZ (Fig. S2). The reasons for this mismatch are unknown, but are likely related to our

800

600

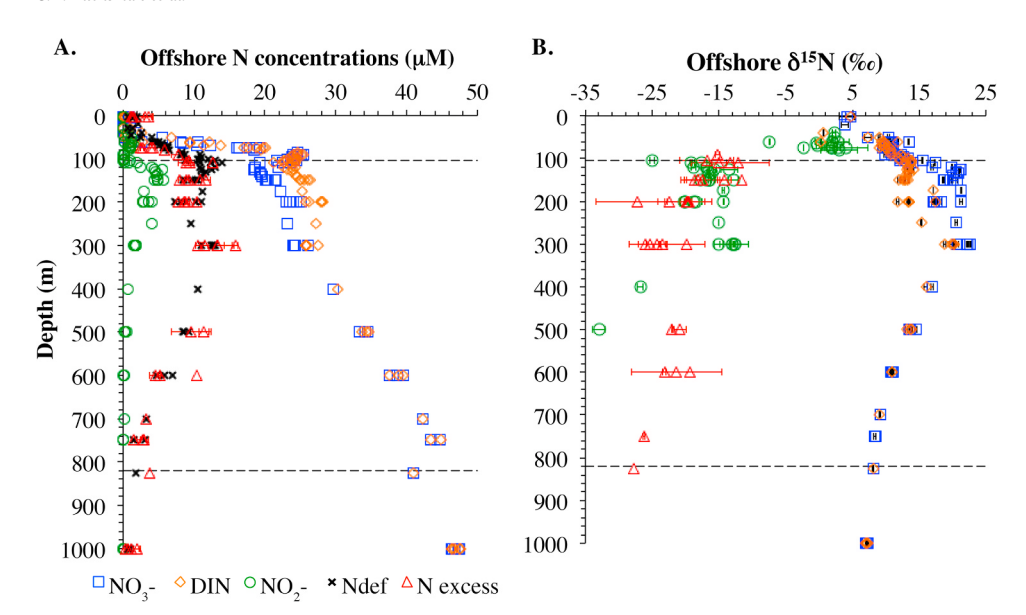


**Fig. 4.** Compilation of ETNP N concentrations (A) and isotopes (B) for offshore stations (St 135–164) plotted versus depth. Dashed lines indicate the boundaries of the ODZ using STOX oxygen electrode measurements from Tiano et al. (2014).

background values imperfectly capturing the actual background due to water mass mixing.

The ETNP  $\delta^{15}$ N-N<sub>2</sub> measurements range from 0.34 to 0.62% and frequently have a minimum < 0.4% at 300 m (Fig. S2). These measurements are similar to  $\delta^{15}$ N-N<sub>2</sub> data from the ETNP in 1993 (Brandes et al., 1998). Measured  $\delta^{15}$ N-N<sub>2</sub> also contains both a biological and background signals. The  $\delta^{15}$ N-N<sub>2</sub> value in seawater at equilibrium with air is about 0.68  $\pm$  0.02% (Knox et al., 1992). Mixing has a much smaller effect on  $\delta^{15}$ N isotopes than on N<sub>2</sub> concentrations since all water masses bear the equilibrium isotope signature. The average  $\delta^{15}$ N-N<sub>2</sub> measurements at 1500 m, a depth not influenced by the ODZ, at the 4 offshore stations (data not shown) was 0.65  $\pm$  0.05%. Here we used 0.68% as our background value, but also made calculations using values of 0.65% and 0.7% in order to estimate potential error in the calculation of  $\delta^{15}$ N-N<sub>2</sub> excess (Fig. S2). The resulting  $\delta^{15}$ N-N<sub>2</sub> excess values for the ETNP were generally between -10% and -30% (Fig. 4 and S2, S4).

Total  $\delta^{15}$ N-N<sub>2</sub> for the Arabian Sea ranged from 0.45‰ to 0.55‰ (Fig. S9). Despite this,  $\delta^{15}$ N-N<sub>2</sub> excess values for the Arabian Sea, calculated as above but using N<sub>2</sub>:Ar<sub>background</sub> calculations from the Arabian Sea (Chang et al., 2012) were between -14‰ and -20‰ (Fig. 5), which is in the same range as the ETNP.

In the ETNP, the  $\delta^{15}$ N-NO $_3^-$  increased from around 10‰ in the oxycline to around 20‰ in the ODZ and then values decreased towards the lower oxycline (Fig. 4). In the Arabian Sea,  $\delta^{15}$ N-NO $_3^-$  was 11–12‰ at the top and bottom of the ODZ, but reached 24‰ in the heart of the ODZ (Fig. S10). The ETNP  $\delta^{15}$ N-NO $_2^-$  was generally in the -15‰ to -20‰ range in the ODZ (Fig. 4 and S2). While  $\delta^{15}$ N-NO $_2^-$  had similar range of values as  $\delta^{15}$ N-NO $_2^-$  excess, at each station  $\delta^{15}$ N-NO $_2$  excess was enriched compared to  $\delta^{15}$ N-NO $_2^-$  in the upper ODZ, but became more depleted than  $\delta^{15}$ N-NO $_2^-$  at 200–300 m (Fig. S2). In the Arabian Sea,  $\delta^{15}$ N-NO $_2^-$  and  $\delta^{15}$ N-NO $_2^-$  started to become more depleted with depth reaching -31‰ at 375 m (Fig. 5).  $\delta^{15}$ N-NO $_2^-$  values from the Arabian Sea ODZ (Fig. 5) are similar to those seen in the ETNP in 2012.

In the ETNP, nitrite concentrations were 5  $\mu$ M offshore and reached 6  $\mu$ M closer to the coast (Fig. 3) which is unusually high for the ETNP (Horak et al., 2016). Accordingly,  $\delta^{15}$ N-NO<sub>2</sub> was different in 2012 than values seen in the ETNP in 2003 (Casciotti and McIlvin, 2007). In 2003,  $\delta^{15}$ N-NO<sub>2</sub> values changed from -15% to -18% at the top of the ODZ to -8% at 300 m (Casciotti and McIlvin, 2007). In contrast, in 2012 the  $\delta^{15}$ N-NO<sub>2</sub> values were more negative at depth than in 2003, with values at 300 m of -12% to -15% (Fig. 4, S2). We suspect that this is due to the higher nitrite concentrations in 2012 than seen in 2003

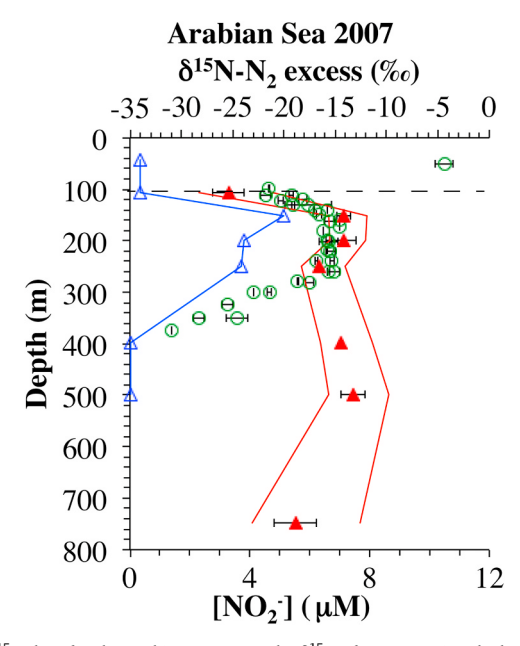


Fig. 5.  $\delta^{15}N$  data for the Arabian Sea St 1. The  $\delta^{15}N$  of  $N_2$  excess is calculated by subtracting background values. Red triangles are  $\delta^{15}N$  of  $N_2$  excess for a background value of 0.68% (Knox et al., 1992). Red lines indicate the range of values if background is varied between 0.65% and 0.7%.  $\delta^{15}N$ -NO $_2$ - is also shown where available (green circles). Nitrite concentrations (lower axis) are shown for comparison (blue triangles). Dashed lines indicate the boundaries of the ODZ.

 $(3.5\,\mu\text{M})$ . It is still unclear why these differences in concentration occurred (Horak et al., 2016), but larger concentrations should buffer the enrichment of the remaining nitrite as it is reduced.

# 3.2. $\Delta^{15}N$ values

A comparison between different N species  $\delta^{15}$ N values helps quantify the importance of oxidation and reduction in the system (Casciotti, 2009; Casciotti et al., 2013).  $\Delta^{15}N_{NO3-NO2}$ , the difference between  $\delta^{15}N_{NO3}$  and  $\delta^{15}N_{NO2}$ , was consistently about 32% through most of the ETNP ODZ, though values may be slightly smaller below 300 m (Fig. 6). Similar results were found in 2003 ETNP data (Fig. 6; Casciotti and McIlvin, 2007). In the Arabian Sea, the  $\Delta^{15}N_{NO3-NO2}$  was  $\sim$  35% at the top of the ODZ but was  $\sim$  40% for the majority of the ODZ (Fig. S10). Interestingly, the  $\Delta^{15}N_{NO3-NO2}$  had significantly more structure in the

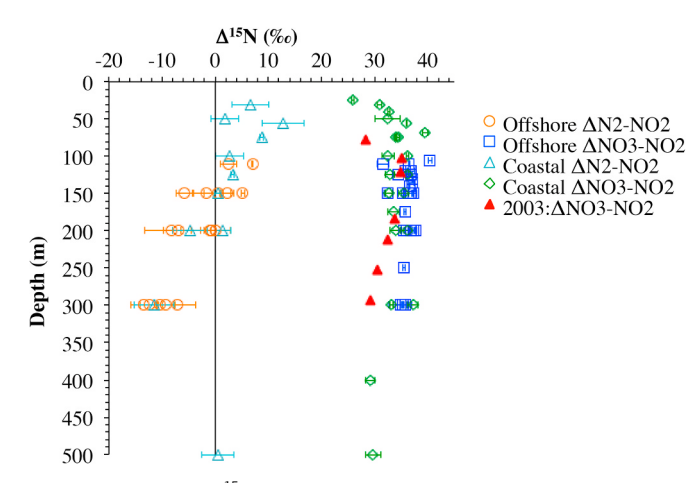


Fig. 6. A compilation of  $\Delta^{15}$ N for the difference between nitrate and nitrite and for the difference between  $N_2$  and nitrite for the secondary nitrite peak at both offshore and coastal stations in the ETNP. All data points are in the ODZ.

ETSP (Casciotti et al., 2013) than seen here in the ETNP and Arabian Seas. The  $\Delta^{15}N_{NO3-NO2}$  values seen here are greater than  $\sim 25\%$ , an upper estimate on the isotope effect ( $\epsilon$ ) value for nitrate reduction (Granger et al., 2008), indicating the influence of nitrite oxidation on the system (Casciotti et al., 2013). Nitrite oxidation has an inverse fractionation effect, which means that the nitrate produced becomes more enriched and the nitrite remaining becomes more depleted (Buchwald and Casciotti, 2010; Casciotti, 2009). Thus, nitrite oxidation can increase the isotopic separation between NO<sub>3</sub> and NO<sub>2</sub>. The more nitrite oxidation the greater the  $\Delta^{15} N_{NO3}$  -NO2 (Casciotti et al., 2013). However, one would expect that nitrite oxidation to be higher at the edges of the ODZ (Babbin et al., 2017; Penn et al., 2016; Peters et al., 2016), and  $\Delta^{15}N_{NO3}$  -NO2 does not follow this trend both for the ETNP and the Arabian Sea (Fig. 6, S10). We also examined  $\Delta^{15}N_{N2-NO2}$ , the  $\delta^{15}N$  difference between excess  $N_2$  and nitrite for the ETNP. These values consistently become more depleted with depth, changing sign from 2% to 10% at the top of the ODZ to -6% to -15% at 300 m (Fig. 6).  $\Delta^{15} N_{N2\text{-}NO2}$  values highlight that  $\delta^{15} N\text{-}N_2$  excess was enriched compared to  $\delta^{15}$ N-NO<sub>2</sub> in the upper ODZ, but became more depleted than  $\delta^{15}$ N-NO<sub>2</sub> at 200–300 m (Fig. 6, S2). The change between positive to negative  $\Delta^{15} N_{N2\text{-}NO2}$  occurs at the nitrite maximum, which is in the 13 °C water mass. Interestingly, the positive  $\Delta^{15}$ N  $_{NO2-N2}$  in the top 50 m of the ODZ indicates that the N<sub>2</sub> produced is more enriched than nitrite even though nitrite is the source of N2 (Fig. 6). Isotope effects for nitrite reduction of  $\varepsilon = 22\%$  have been found in bacterial cultures containing the copper-type nitrite reductase (NirK) and  $\varepsilon = 8\%$  in cultures containing the heme-type nitrite reductase (NirS) (Martin and Casciotti, 2016). In an eddy in the ETSP, the isotope effect for nitrite reduction was calculated to be 12‰ (Bourbonnais et al., 2015), similar to cultures with the NirK copper nitrite reductase (Martin and Casciotti, 2016). However, in situ nitrite data has been successfully modeled with no fractionation during nitrite reduction in the Southern ETNP (Buchwald et al., 2015) and ETSP (Casciotti et al., 2013; Peters et al., 2016), and  $\delta^{15}$ N-NO<sub>2</sub> and  $\delta^{15}$ N-N<sub>2</sub> excess values were nearly identical in the Arabian Sea (Fig. 5). Scenarios to explain this data are discussed below (Section 4.3).

# 3.3. Isotope effect for $N_2$ production

To minimize the complication of nitrite oxidation on our calculations, we combine  $\delta^{15}\text{N-NO}_2$ , and  $\delta^{15}\text{N-NO}_3$  to form  $\delta^{15}\text{N-DIN}$ . We calculated the closed system fractionation effect for  $N_2$  production from  $\delta^{15}\text{N-DIN}$  and from  $\delta^{15}\text{N}$  of biologically produced  $N_2$  ( $\delta^{15}\text{N-N}_2$  excess). Closed system calculations assume no re-supply of substrate, in this case nitrate, so are appropriate where there is little mixing (Hu et al., 2016).

As our stations were far removed from the edges of the ODZ where mixing and re-supply of nitrate would occur (Fig. 2), we chose a closed system isotope effect calculation. Individual isotope effects were calculated for each sample using the equations for closed system fractionation (Mariotti et al., 1981):

$$\delta^{15}DIN = \delta^{15}DIN_{initial} + \varepsilon \times \ln[f]$$
(4)

$$\delta^{15}N_{2,\text{excess}} = \delta^{15}DIN_{initial} - \varepsilon \left(\frac{f}{1-f}\right) \ln [f]$$
(5)

where  $\epsilon$  is the isotope effect and f is the fraction of DIN remaining. In all cases, values for f were calculated as:

$$f = \frac{NO_3^- + NO_2^-}{DIN_{expected}} \tag{6}$$

where

$$DIN_{expected} = NO_3^- + NO_2^- + N_{2,excess}$$
 (7)

Thus, instead of calculating expected DIN based on an assumed N:P ratio, N<sub>2.excess</sub> measurements were used to quantify the amount of DIN removed. The isotope effect for nitrate reduction was calculated similarly to DIN. Also, instead of assuming a deep water value for  $\delta^{15}$ N- $\text{DIN}_{\text{initial}},$  we calculated  $\delta^{15}\text{N-DIN}_{\text{initial}}$  by combining the mass-weighted isotopes of nitrate, nitrite, and N2 excess (Fig. S11) which contains the influence of remineralized organic matter as well as the original nitrate. In the ODZ, we assumed that remineralized organic matter is converted to N2 via anammox. For this calculation, we assumed that N2 fixation rates were negligible. Offshore nitrogen fixation rates measured in the ODZ on this cruise were 0.2 nM per day (Jayakumar et al., 2017), supporting this assumption. We did not include N<sub>2</sub>O in this calculation, but N<sub>2</sub>O concentrations were from 0 to 60 nM in the ODZ for this cruise (Babbin et al., 2015), so were insignificant to the calculation when mass-weighted. Ammonium concentrations were also generally below detection in the ODZ (Fig. S3; Peng et al., 2015). Averaging across all samples yielded  $\delta^{15} \text{N-DIN}_{initial}$  of 5.3  $\pm$  0.8% for the ETNP and  $5.6\% \pm 0.9\%$  for the Arabian Sea. These average values were used as  $\delta^{15} \text{N-DIN}_{initial}$  in our calculations. Our average  $\delta^{15} \text{N-DIN}_{initial}$  values of 5.3% and 5.6% are very similar to those used in previous isotope effect calculations in the ETSP (5.5%; Bourbonnais et al., 2015; Hu et al., 2016). However, more enriched  $\delta^{15}$ N-NO<sub>3</sub> values have been found for the intermediate waters at station ALOHA (6.4%; Sigman et al., 2009) and in the 200-600 m Pacific equatorial waters (7%; Rafter et al., 2013). Thus  $\delta^{15}\mbox{N-DIN}_{\mbox{initial}}$  in the ODZ is more depleted than nitrate in the ODZ source waters. By using this calculated  $\delta^{15}$ N-DIN<sub>initial</sub> based on our data, we avoid the over estimation of the N2 production isotope effect due to aerobic respiration as discussed by Marconi et al. (2017). If δ15N-DIN<sub>initial</sub> were chosen from source waters, the addition of remineralized organic N would be incidentally included in the isotope effect calculation (Marconi et al., 2017). In fact, given the relatively enriched source waters, it does appear that our depleted  $\delta^{15}$ N-DIN<sub>initial</sub> values are probably due to the influence of remineralization. Sediment trap samples from our ETNP cruise had a  $\delta^{15}$ N of 8.1  $\pm$  0.4% offshore (n = 2) and 8.7  $\pm$  0.4% onshore (n = 5) (Table S2; Rick Keil, personal communication). Due to little seasonality in the chlorophyll a, productivity, and nitrate supply in our region of the ETNP (Pennington et al., 2006), we assume that the isotopic composition of our sediment trap samples were representative. Sediment trap material from the Arabian Sea 2007 ODZ (collection described in Keil et al., 2016) had  $\delta^{15}$ N of 7 ± 1‰ (n = 12; Table S2; Rick Keil, personal communication), similar to values from the ETNP. Given a isotope effect for organic matter remineralization to ammonium of 4% (Macko et al., 1994; Saino and Hattori, 1980; Wada, 1980), remineralized N should have been  $\sim 4$  to 5‰ in the ODZ, similar to our  $\delta^{15}$ N-DIN<sub>initial</sub> of 5.3  $\pm$  0.8‰ or  $5.6 \pm 0.9\%$ .

When calculated for each depth, the closed isotope effects for the ETNP derived from DIN and  $N_2$  excess match closely; they are -20 to

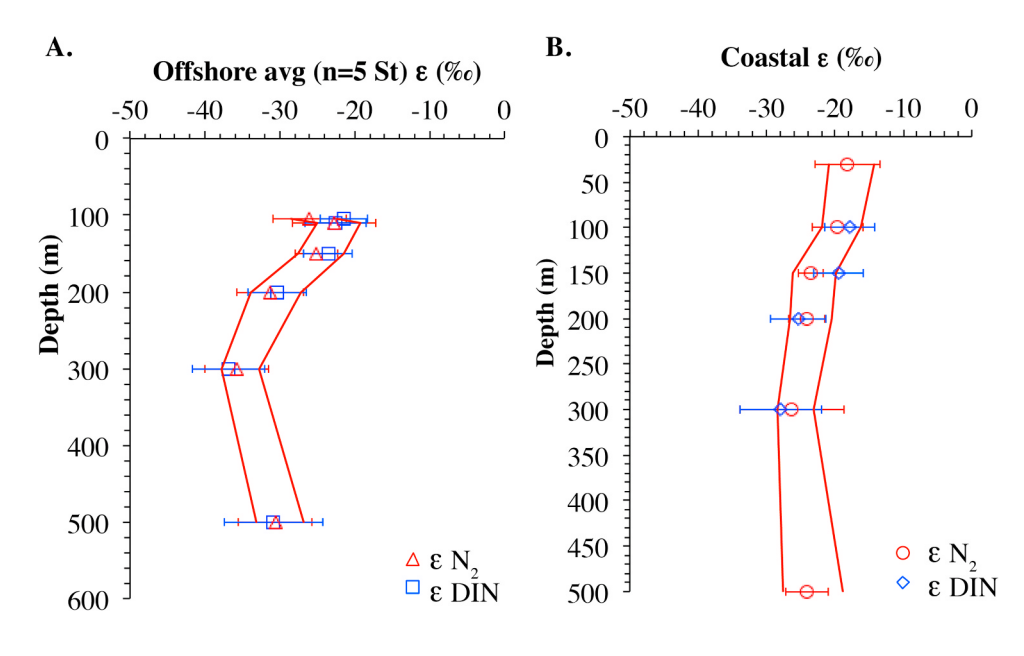


**Fig. 7.** Variability of the isotope effect (ε) for  $N_2$  production ( $\delta^{15}$ N-DIN or  $\delta^{15}$ N-N<sub>2</sub> excess) with depth in the ETNP at A) an average of offshore stations 135–164 (individual stations can be seen in Fig. S12) and B) at coastal station 132 (bottom depth 550 m). Red lines indicate what the fractionation factor would be if the background was shifted from 0.68‰ (Knox et al., 1992) to either 0.65‰ or 0.7‰.

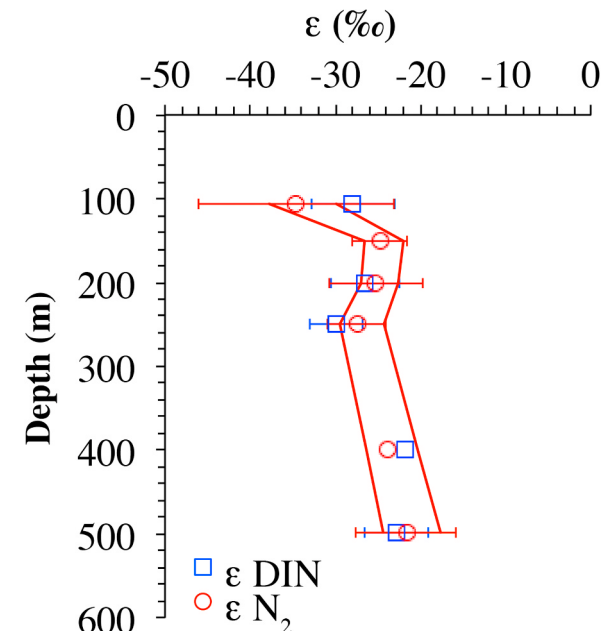


**Fig. 8.** Closed system fractionation factors for the Arabian Sea in 2007. Red lines indicate what the fractionation factor would be if the background was shifted from 0.68% (Knox et al., 1992) to either 0.65% or 0.7%.

-25% at the top of the ODZ, increase to -30 to -45% at  $\sim300$  m, and then decrease again toward the bottom of the ODZ (Fig. 7, and S12). In the Arabian Sea, the closed isotope effects derived from DIN and  $N_2$  excess were fairly constant, varying between -24% and -30% (Fig. 8). As expected, in both the ETNP and the Arabian Sea,  $\delta^{15} N\text{-NO}_2$  was often most depleted at the top of the ODZ, where one would expect nitrite oxidation (Fig. 5, and S2). However, unlike the Arabian Sea, where  $\delta^{15} N\text{-NO}_2$  and  $\delta^{15} N\text{-N}_2$  are closely correlated for the top 300 m and  $\delta^{15} N\text{-N}_2$  is fairly constant with depth (Fig. 5), in the ETNP,  $\delta^{15} N\text{-N}_2$  excess does not track  $\delta^{15} N\text{-NO}_2$ , and  $\delta^{15} N\text{-N}_2$  excess has the most depleted values in 250–300 m range towards the bottom of the SNM (Fig. 4, S2, S4). Unsurprisingly, 250–300 m is the same range where the isotope effects are the largest (Fig. 7, Fig S12).

For the ETNP, the average apparent closed isotope effect for consumption of DIN was  $-26\pm11\%$  (using Eq. (4)) and it was  $-27\pm6\%$  for production of  $N_2$  excess (using Eq. (5)). The closed isotope

effect from St 132, our ETNP coastal station ( $-23\pm3\%$  for  $N_2$  and  $-23\pm5\%$  for DIN; 550 m bottom depth; Fig. 7), is similar to our offshore average value ( $-29\pm5\%$  for  $N_2$ ). If the closed isotope effect for the ETNP was calculated by the more traditional Rayleigh plot, the values were quite similar to our average depth calculations (-25.1% for DIN; Figure S13), but due to the previously mentioned variability with depth, the  $R^2$  value was only 0.5 for DIN and was worse for  $N_2$  gas (data not shown). Though we prefer a closed system calculation, we also examined our results with an open system calculation where mixing is assumed to be a dominant process:

$$\delta^{15}DIN = \delta^{15}DIN_{initial} + \varepsilon \times (1 - f)$$
(8)

$$\delta^{15}N_{2,\text{excess}} = \delta^{15}DIN_{initial} - \varepsilon \times f. \tag{9}$$

Our isotope effects were similar, though more variable, if an open system calculation was used ( $-29\pm17\%$  for DIN and  $-32\pm8\%$  for  $N_2$  in the ETNP). This similarity between closed and open systems supports the robustness of our calculations. Given that the N deficit (calculated from nutrients) and the  $N_2$  excess (calculated from  $N_2$  gas) were quite similar (Fig. 4, S2, S4, S8), as were the isotope effects calculated from reactants and from the product, we assume that we have mass balance in our system.

The Arabian Sea is another major ODZ. We have  $\delta^{15} \text{N-N}_2$  excess and  $\delta^{15}$ N-DIN from one offshore station from Arabian Sea in 2007 (R/V Revelle) (Fig. 5). Sediment trap material from the Arabian Sea 2007 ODZ (Keil et al., 2016) had  $\delta^{15}$ N of 7 ± 1% (n = 12; Table S2; Rick Keil, personal communication), similar to values from the ETNP. Thus it is not surprising that  $\delta^{15}$ N-DIN<sub>initial</sub> was also similar (5.6%  $\pm$  0.9%). When δ<sup>15</sup>N-N<sub>2</sub> is examined from the Arabian Sea, the closed isotope effect was 26  $\pm$  4‰ and the isotope effect for  $\delta^{15}$ N-DIN was 26  $\pm$  3‰ (Fig. 8), which is also similar to the offshore ETNP. These numbers are significantly larger than those determined from the coastal ETSP data (Hu et al., 2016) but are consistent with older  $\delta^{15}$ N-DIN data from the Arabian Sea in 1993, 1994, and 1995 ( $\varepsilon = 22 \pm 3\%$  with a  $\delta^{15}$ N-DI- $N_{initial}$  of 6% and  $\epsilon=$  24.24% with  $\delta^{15} N\text{-DIN}_{initial}$  of 5%) and from the ETNP in 1993 ( $\epsilon = 25 \pm 2\%$  with a  $\delta^{15}$ N-DIN<sub>initial</sub> of 6%) and from the ETNP in 1997 ( $\varepsilon = 22.5\%$  with a  $\delta^{15}$ N-DIN<sub>initial</sub> of 6.2%) (Brandes et al., 1998; Voss et al., 2001). Combined, this data indicates that the isotope effect for N2 production is similar for the offshore regions of these two ODZs and is approximately 25%.

The isotope effect for nitrate reduction in the ETNP was  $-28 \pm 6\%$ , which was in the same range as the isotope effect for DIN. In Arabian Sea the isotope effect for nitrate reduction was  $-25 \pm 6\%$ ,

also in the same range as the isotope effect for DIN. This differs from the ETSP where isotope effect for nitrate reduction has been repeatedly found to be significantly larger than that for DIN conversion to  $N_2$  (Bourbonnais et al., 2015; Casciotti et al., 2013; Peters et al. this issue).

#### 4. Discussion

The Eastern Tropical North Pacific (ETNP) ODZ is the largest marine ODZ by volume and accounts for ~ 40% of marine anoxic waters by area (Paulmier and Ruiz-Pino, 2009). At offshore stations in the core of the ODZ in 2012, oxygen was below detection for a STOX sensor from 105 m to 800 m. Both rates of N<sub>2</sub> production by denitrification and anammox were measured in incubation experiments during this cruise (Babbin et al., 2015, 2014) and the addition of sediment trap material stimulated denitrification rates (Babbin et al., 2014). Denitrifier RNA has been found to be enriched within particles in the ETNP (Ganesh et al., 2015). The Arabian Sea only accounts for 8% of marine anoxic waters by area, but thickness of the ODZ is comparable to the ETNP (Paulmier and Ruiz-Pino, 2009). On our cruise in the Arabian Sea in 2007, denitrification rates and genes dominated over anammox (Ward et al., 2009) and the addition of sediment trap material stimulated denitrification rates (Chang et al., 2014).  $N_2$  gas and  $\delta^{15}N$ ,  $\delta^{15}N$ - $NO_2$ and  $\delta^{15} \text{N-NO}_3^-$  were measured along a coast to open ocean transect in core of the ETNP ODZ and on one station in the Arabian Sea. Interestingly in the ETNP,  $\Delta^{15}N$   $_{\rm NO2\text{-}N2}$  changed with a clear trend from negative to positive with depth and the isotope effects for N2 production also changed with depth. These same features were not seen in the Arabian Sea. In both the ETNP and Arabian Sea, the isotope effects calculated from DIN and N2 were quite similar, and the magnitude of the isotope effect was large.

#### 4.1. Change in isotope effect with depth

In the ETNP, the absolute values of the apparent isotope effects for DIN and  $N_2$  excess increase with depth until  $\sim 300$  m and then decrease again (Fig. 7, S12). This same change in isotope effects with depth is not seen in the Arabian Sea (Fig. 8). Instead in the Arabian Sea there is a slight decrease in apparent isotope effect with depth (Fig. 8). Below we discuss 6 possible explanations for this observation in the ETNP. One hypothesis to explain this could be the influence of nitrite oxidation at the top of the ODZ.  $\delta^{15}$ N-NO<sub>3</sub> and  $\delta^{15}$ N-NO<sub>2</sub> values from the Southern ETNP (Costa Rica Dome) were similar to values presented here and could be modeled completely by nitrate and nitrite reduction, with nitrite oxidation (Buchwald et al., 2015) but N2 gas was not included in the model. Nitrite oxidation could affect the system by modifying  $\delta^{15}$ N- $NO_2$ , and  $\delta^{15}N-NO_3$  and by affecting the nitrite concentrations. Isotope effects are often reduced at low substrate concentrations. However, the DIN and N<sub>2</sub> excess isotope effects are largest at 250-300 m where nitrite concentrations are already greatly reduced, so nitrite concentrations cannot explain the isotope effect depth profile. Additionally, nitrite oxidation would affect the intermediate reactant  $\delta^{15}$ N-NO<sub>2</sub>-, which could then affect  $\delta^{15} \text{N-N}_2$  and the isotope effect. However,  $\delta^{15} \text{N-NO}_2\text{-}$ and  $\delta^{15}$ N-N<sub>2</sub> excess do not correlate in the 250–300 m region, implying a different cause for the change in isotope effect. All together, nitrite oxidation does not appear to be responsible for the change in isotope effects with depth.

A second hypothesis would involve the input of ammonium into the ODZ from migrating micronekton/zooplankton. ADCP data indicates micronekton migrate to 300 m in the ETNP (Bianchi et al., 2014).  $\delta^{15} N$  of ammonium from excretion under ODZ conditions is not well quantified. Theoretically, the input of depleted ammonium from zooplankton at 300 m could affect  $\delta^{15} N\text{-}N_2$  gas, making it more depleted. However, any significant depletion from injected ammonium would also appear in our DIN\_initial calculations, and it does not (Figure S11).

A third hypothesis is that the differences in isotope effects are due to differences in physical processes. The T/S diagram (Fig. S5), shows that

the nitrite maximum is in the Pacific Equatorial 13 °C water (Fiedler and Talley, 2006). The anoxic water masses above and below could carry different signals that would then mix. Theoretically, the calculated DIN fractionation effect in the 13 °C water could be affected by mixing with oxic water above it (Marconi et al., 2017). In fact, the enriched  $\delta^{15}\text{N-NO}_3^-$  in the oxycline above the ODZ (Fig. 4) suggests that mixing is occurring. However, calculation errors from this mixing would be, once again, related to incorrect choice of  $\delta^{15}\text{N-DIN}_{\text{initial}}$ . Since our  $\delta^{15}\text{N-DIN}_{\text{initial}}$  (Section 4.2) and DIN $_{\text{expected}}$  (Eq. (7)) are calculated from our DIN and  $N_2$  data without assumptions that could vary with water mass, it remains unclear why the different water masses would have different fractionation effects.

Because the  $\Delta^{15}N_{NO3}$  -NO2 has little variability from the top of the ODZ to 300 m while  $\Delta^{15}$ N <sub>NO2-N2</sub> changes with a clear trend (Fig. 6), it seems possible that the change in isotope effect for N2 production with depth has to do with nitrite reduction. A fourth hypothesis to explain the difference in isotope effects with depth would be a change in the N2 producing bacterial community at 200-400 m. Different types of bacteria are known to have different nitrite reduction isotope effects based on their type of nitrite reductase (Martin and Casciotti, 2016). However, nirK was the dominant nitrite reductase gene throughout the ODZ (Fuchsman et al., 2017) and  $\Delta^{15}N_{NO2-N2}$  values were positive in the upper ODZ and negative below, switching sign at the nitrite maximum. It seems unlikely that some bacteria would have a positive isotope effect for nitrite reduction and other bacteria would have a negative nitrite reduction isotope effect. However, it is possible that some denitrifiers could use nitrate as an oxidant, and keep and use the nitrite produced internally, while others use nitrite from the bulk water column. Given the large difference in  $\delta^{15}N$  between nitrate and nitrite, these two hypothetical types of bacteria would produce very different δ<sup>15</sup>N-N<sub>2</sub>. For example, at 100 m a denitrifying bacterium using nitrate would start with a reactant at  $\sim 12\%$  while a bacterium using nitrite would start with a reactant at  $\sim -18\%$ . For the nitrate case, an isotope effect of  $\sim 20\%$  would explain the  $\delta^{15}$ N-N<sub>2</sub> excess (- 12 to -18‰) at 100 m while the nitrite case would need a reverse isotope effect. However, at 300 m, nitrate is 20% while nitrite is - 14 to -16‰. Thus a nitrite reduction isotope effect of 10‰ would successfully explain  $\delta^{15}$ N-N<sub>2</sub> excess (~ - 26‰) at 300 m while an isotope effect from nitrate would be exceptionally large (46%). It appears that a switch in the type of denitrifier could reproduce our measurements. What is unclear is if these two types of bacteria actually exist. In gram negative bacteria, nitrite reduction occurs in the periplasm (Zumft, 1997), where nitrite can escape the cell across the outer membrane. However, an internal nitrite pool has been demonstrated for denitrifying bacteria in a sulfidic fjord (Jensen et al., 2009). The hypothesis is that if a bacterium performs both nitrate reduction and nitrite reduction, some nitrite may escape the cell, but the nitrite concentrations inside the cell is still higher than its surroundings (Jensen et al., 2009). Additionally, the use of an internal nitrite pool for at least some denitrifiers has been suggested previously in the ETSP and Arabian Seas to explain excess  $\delta^{29}N_2$  produced in enriched  $^{15}N$  experiments with nitrite (Chang et al., 2014; De Brabandere et al., 2014).

Additionally the apparent isotope effects for nitrate and nitrite reduction could be reduced at the top of the ODZ due to assimilation. Cyanobacteria photosynthesize at the top of the ODZ in the ETNP (Garcia-Robledo et al., 2017), so are presumably assimilating nitrogen in some form. Assimilation has a small isotope effect of 5–7‰ (Altabet, 2001; Granger et al., 2004) and so could be reducing the combined apparent isotope effect at the top of the ODZ. However, neither assimilation of nitrate nor of nitrite can explain the  $\Delta^{15} N_{\rm NO2-N2}$  changes in sign.

Finally, denitrifiers are known to be attached to particles (Fuchsman et al., 2017; Ganesh et al., 2015, 2014). Given sediment trap data ( $\delta^{15}N$  of organic N of 8‰), in the ETNP, and with a isotope effect for organic matter remineralization to ammonium of 4‰ (Macko et al., 1994; Saino and Hattori, 1980; Wada, 1980), nitrite produced from

remineralized ammonium within particles would be enriched compared to the highly depleted, water column nitrite measurements. Low levels of particle associated nitrite has been found in oxic waters at Station ALOHA (Wilson et al., 2014). The presence of nitrite has been showed to stimulate N2O production in particles at Station ALOHA (Wilson et al., 2014). Theoretically,  $N_2$  could also be produced from nitrite in particles. Nitrite can only be produced from particle remineralization when some oxygen is available. Thus, as the presence of even trace amounts of oxygen diminishes with depth, more enriched N2 produced from remineralized nitrite in particles would also decrease. In this case a bacterium using remineralized nitrite in a particle would start with a reactant at ~4‰. As the proportion of N<sub>2</sub> produced with this remineralized nitrite decreased with depth, utilization of depleted water column nitrite would become dominant. For example, a simple calculation using St 161 as a template (Fig S2), assuming water column nitrite of -16%, and  $N_2$  excess of -12% at the top of the ODZ with a constant nitrite reduction isotope of effect of 10%, approximately 70% of nitrite reduced would need to be from particles (producing N2 at -6%) and  $\sim 30\%$  from the water column (producing N<sub>2</sub> at -26%). While at 300 m, the measured  $N_2$  excess (-25%) could be reproduced by using 100% water column nitrite. This hypothesis could explain the apparent change in isotope effect with depth along with changes in  $\Delta^{15}$ N  $_{NO2-N2}$  values. Additionally, the large use of remineralized organic matter in this scenario would also be consistent with our calculated 5.3% DIN<sub>initial</sub> values, which reflect remineralization.

While nitrite oxidation, migrating zooplankton and mixing between water masses undoubtedly occur in the ODZ and may affect our isotope values, alone they cannot explain our variability in isotope effects. However, both a shift between denitrifiers with and without an internal nitrite pool or denitrification inside sinking particles can explain our ETNP data.

#### 4.2. Magnitude of $N_2$ production isotope effect

Lately, evidence has mounted for a small fractionation effect (< 15‰) for water column denitrification. This small fractionation effect is based on culture experiments and isotopic data from the ETSP (Bourbonnais et al., 2015; Casciotti et al., 2013; Hu et al., 2016; Kritee et al., 2012). However, our data from the heart of the ETNP indicates a large apparent isotope effect of 26 ± 11%, calculated from DIN, or 27 ± 6‰, calculated from N<sub>2</sub> excess. Similarly our data from the Arabian Sea also indicated a large apparent closed isotope effect of  $26 \pm 4\%$  from  $\delta^{15}$ N-N<sub>2</sub> excess and  $26 \pm 3\%$  for  $\delta^{15}$ N-DIN. Our result also contrasts with isotope effect calculations derived from DIN data collected on in the ETSP ODZ, which ranged from 11% to 14% (Bourbonnais et al., 2015; Hu et al., 2016). Additionally, nitrate reduction and DIN isotope effects are similar in the ETNP and Arabian Sea, but have been repeatedly found to differ in the ETSP (Bourbonnais et al., 2015; Casciotti et al., 2013; Peters et al., in this issue). The isotope effect calculation is extremely sensitive to the fraction remaining, which often depends on phosphate in N deficit calculations, but Hu et al. (2016), Bourbonnais et al. (2015), and our calculations avoid this issue by using measured N2 excess instead of N deficit in the fraction remaining calculations. The difference between our isotope effects and published isotope effects from the ETSP could be due to differences associated with the location of sampling in those studies. One of the ETSP studies was coastal with bottom depths less than 150 m (Hu et al., 2016) and the other two were from eddies influenced by coastal water (Altabet et al., 2012; Bourbonnais et al., 2015). Nitrate concentrations were greatly reduced on these study sites compared to our stations (Altabet et al., 2012; Bourbonnais et al., 2015; Hu et al., 2016). On the coastal ETSP transect, there were mismatches between N2 excess and N deficit (Hu et al., 2016). Data from an along shore transect in the ETSP in 2013 also found mismatches between N2 excess and N deficit at some stations (Peters et al., this issue). The coastal ETSP shelf, where  $\delta^{15}$ N-N<sub>2</sub> excess was examined, was affected by sediments (Hu et al., 2016),

which have near zero isotope effects (Brandes and Devol, 1997; Lehmann et al., 2007). Perhaps, due to the larger width of the Peru shelf (Smith and Sandwell, 1997; visualization on <a href="http://topex.ucsd.edu/marine\_topo">http://topex.ucsd.edu/marine\_topo</a>), sedimentary processes influence the isotope effects in this region. Our coastal station from the ETNP did not have reduced isotope effects compared to the offshore ETNP (Fig. 7). However, the ETNP shelf in the region sampled was quite narrow (Smith and Sandwell, 1997). It seems that the ETSP system is more complicated in some way than the ETNP and Arabian Sea, which affects the apparent isotope effects calculated there.

Our DIN and  $N_2$  excess isotope effects are apparent isotope effects that include both denitrification and anammox. However, our nitrate reduction isotope effects for the ETNP ( $-28\pm6\%$ ), and Arabian Sea ( $-25\pm6\%$ ) were also large. In culture, dentirifiers grown at slow rates to mimic the estimated in situ water column rates exhibit small nitrate reduction fractionation effects (Kritee et al., 2012). However, cultures grown at high rates show large fractionation effects (Granger et al., 2008; Kritee et al., 2012). Mounting evidence suggests that denitrifiers are preferentially partitioned onto particles (Fuchsman et al., 2017; Ganesh et al., 2015, 2014). In all three ODZs, denitrification rates were high when sinking particles were included (Babbin et al., 2014; Chang et al., 2014). This suggests that much of the denitrification in the ODZ may be taking place at higher growth rates associated with particles and therefore, with a larger fractionation effect.

#### 4.3. Implications

The balance between sedimentary denitrification and water column denitrification sets the  $\delta^{15}N$  of oceanic nitrate. Assuming that in general sedimentary denitrification has a very small fractionation effect, a small the water-column isotope effect for denitrification allows the calculation of a lower the sedimentary denitrification rate (Altabet, 2007; Brandes and Devol. 2002: DeVries et al., 2012). We find evidence for relatively large isotope effects in all three ODZs implying correspondingly large sedimentary denitrification rates. If the ocean is at steady state, denitrification and N2 fixation should balance, and have been modeled to do so (DeVries et al., 2013, 2012). However, the balance between denitrification and N2 fixation also depends on N2 fixation rates, values for which are presently in a state of flux (Konno et al., 2010; Mohr et al., 2010; Moisander et al., 2010). Older N2 fixation rates calculated from <sup>15</sup>N additions are likely to be underestimates due to problems with the measurement (Konno et al., 2010; Mohr et al., 2010). Additionally, new N2 fixing organisms with a greater geographic range have been discovered (Moisander et al., 2010), increasing the area for potential N2 fixation. Correction for these issues may almost double N2 fixation rates (Großkopf et al., 2012). Due to the current uncertainty in N<sub>2</sub> fixation estimates, even the large fractionation effects calculated here do not preclude a balanced N budget (DeVries et al., 2012).

# Acknowledgements

We thank Matthew Forbes for technical assistance with the nitrate and nitrite isotope analyses. We thank Steve Emerson and Paul Quay for use of their lab space and facilities, and to Johnny Stutsman, Mark Haught, and Chuck Stump for assistance during the  $\rm N_2$  gas measurement process. Thank you to the captains and crew of the R/V Thompson and Revelle, and to co-Chief Scientist B.B. Ward. We thank Rick Keil for  $\delta^{15} \rm N$  of sediment trap material, and Aaron Morello for shipboard nutrient analyses. Thanks to Justin Penn for discussions.

This work was supported by the US National Science Foundation OCE 1029316 and OCE-0647981 to AHD and OCE 1140404 to KLC. BXC was partially funded by the Joint Institute for the Study of the Atmosphere and Ocean (JISAO) under NOAA Cooperative Agreement NA100AR4320148 (2010–2015) and NA150AR4320063 (2015–2020), Contribution no. 2017-072. This is NOAA-PMEL contribution no. 4633. The authors gratefully thank SCOR WG 144 and the SCOR, the CSIR and

Ministry of Earth Sciences, Government of India for financial support for the International Symposium on Ocean Deoxygenation at the CSIR-NIO, Goa held during Dec 02-06, 2016.

#### **Funding**

This work was supported by the National Science Foundation (grant numbers: OCE-1029316, OCE-0647981 and OCE 1140404).

#### Appendix A. Supporting information

Supplementary data associated with this article can be found in the online version at https://dx.doi.org/10.1016/j.dsr2.2017.12.013.

#### References

- Altabet, M.A., 2007. Constraints on oceanic N balance/imbalance from sedimentary 15N records. Biogeosciences 4, 75–86.
- Altabet, M.A., 2001. Nitrogen isotopic evidence for micronutrient control of fractional NO<sub>3</sub> utilization in the equatorial Pacific. Limnol. Oceanogr. 46, 368–380. http://dx.doi.org/10.4319/lo.2001.46.2.0368.
- Altabet, M.A., Ryabenko, E., Stramma, L., Wallace, D.W.R., Frank, M., Grasse, P., Lavik, G., 2012. An eddy-stimulated hotspot for fixed nitrogen-loss from the Peru oxygen minimum zone. Biogeosciences 9, 4897–4908. http://dx.doi.org/10.5194/bg-9-4897-2012.
- Babbin, A.R., Bianchi, D., Jayakumar, A., Ward, B.B., 2015. Rapid nitrous oxide cycling in the suboxic ocean. Science 348, 1127–1129. http://dx.doi.org/10.1126/science.
- Babbin, A.R., Keil, R.G., Devol, A.H., Ward, B.B., 2014. Organic matter stoichiometry, flux, and oxygen control nitrogen loss in the ocean. Science 344, 406.
- Babbin, A.R., Peters, B.D., Mordy, C.W., Widner, B., Casciotti, K.L., Ward, B.B., 2017. Novel metabolisms support the anaerobic nitrite budget in the Eastern Tropical South Pacific. Glob. Biogeochem. Cycles 31, 258–271. http://dx.doi.org/10.1002/ 2016GB005407.
- Bianchi, D., Babbin, A.R., Galbraith, E.D., 2014. Enhancement of anammox by the excretion of diel vertical migrators. Proc. Natl. Acad. Sci. USA 111, 15653–15658. http://dx.doi.org/10.1073/pnas.1410790111.
- Bohlke, J.K., Mroczkowski, S.K., Coplen, T.B., 2003. Oxygen isotopes in nitrate: new reference materials for O-18: O-17: O-16 measurements and observations on nitratewater equlibration. Rapid Commun. Mass Spectrom. 17, 1835–1846.
- Bourbonnais, A., Altabet, M.A., Charoenpong, C.N., Larkum, J., Hu, H., Bange, H.W., Stramma, L., 2015. N-loss isotope effects in Peru oxygen minimum zone studied using a mesoscale eddy as a natural tracer experiment. Glob. Biogeochem. Cycles 29, 793–811. http://dx.doi.org/10.1002/2014GB005001.
- Brandes, J.A., Devol, A.H., 2002. A global marine-fixed nitrogen isotopic budget: implications for Holocene nitrogen cycling. Glob. Biogeochem. Cycles 16, 1120. http://dx.doi.org/10.1029/2001GB001856.
- Brandes, J.A., Devol, A.H., 1997. Isotope fractionation of oxygen and nitrogen in coastal marine sediments. Geochim. Cosmochim. Acta 61, 1793–1801.
- Brandes, J.A., Rd, B.B., Devol, H., 1998. Isotopic composition of nitrate in the central Arabian Sea and eastern North Pacific: a tracer for mixing and nitrogen cycles. Limnol. Oceanogr. 43, 1680–1689.
- Bristow, L.A., Dalsgaard, T., Tiano, L., Mills, D.B., Bertagnolli, A.D., Wright, J.J., Hallam, S.J., Ulloa, O., Canfield, D.E., Peter, N., Thamdrup, B., 2016. Ammonium and nitrite oxidation at nanomolar oxygen concentrations in oxygen minimum zone waters. Proc. Natl. Acad. Sci. USA 113, 10601–10606. http://dx.doi.org/10.1073/pnas. 1600359113.
- Brunner, B., Contreras, S., Lehmann, M.F., Matantseva, O., Rollog, M., Kalvelage, T., Klockgether, G., Lavik, G., Jetten, M.S.M., Kartal, B., Kuypers, M.M.M., 2013. Nitrogen isotope effects induced by anammox bacteria. Proc. Natl. Acad. Sci. USA 110, 18994–18999. http://dx.doi.org/10.1073/pnas.1310488110.
- Buchwald, C., Casciotti, K.L., 2010. Oxygen isotopic fractionation and exchange during bacterial nitrite oxidation. Limnol. Oceanogr. 55, 1064–1074.
- Buchwald, C., Santoro, A.E., Stanley, R.H.R., Casciotti, K.L., 2015. Nitrogen cycling in the secondary nitrite maximum of the eastern tropical North Pacific off Costa Rica. Glob. Biogeochem. Cycles 29, 2061–2081. http://dx.doi.org/10.1002/2015GB005187.
- Casciotti, K., Bohlke, J., McIlvin, M., Mroczkowski, S.J., Hannon, J., 2007. Oxygen isotopes in nitrite: analysis, calibration, and equilibration. Anal. Chem. 79, 2427–2436.
- Casciotti, K.L., 2009. Inverse kinetic isotope fractionation during bacterial nitrite oxidation. Geochim. Cosmochim. Acta 73, 2061–2076. http://dx.doi.org/10.1016/j.gca. 2008.12.022.
- Casciotti, K.L., Buchwald, C., Mcilvin, M., 2013. Implications of nitrate and nitrite isotopic measurements for the mechanisms of nitrogen cycling in the Peru oxygen deficient zone. Deep. Res. Part I 80, 78–93. http://dx.doi.org/10.1016/j.dsr.2013.05.
- Casciotti, K.L., McIlvin, M.R., 2007. Isotopic analyses of nitrate and nitrite from reference mixtures and application to Eastern Tropical North Pacific waters. Mar. Chem. 107, 184–201. http://dx.doi.org/10.1016/j.marchem.2007.06.021.
- Casciotti, K.L., Sigman, D.M., Hastings, M.G., Bohlke, J.K., Hilkert, A., 2002.
  Measurement of the oxygen isotopic composition of nitrate seawater and freshwater using the dentirifier method. Anal. Chem. 74, 4905–4912. http://dx.doi.org/10.

- 1021/ac020113w.
- Chang, B.X., Devol, A.H., Emerson, S.R., 2012. Fixed nitrogen loss from the eastern tropical North Pacific and Arabian Sea oxygen deficient zones determined from measurements of  $N_2$ :Ar. Glob. Biogeochem. Cycles 26http://dx.doi.org/10.1029/2011GB004207. (GB004207).
- Chang, B.X., Devol, A.H., Emerson, S.R., 2010. Denitrification and the nitrogen gas excess in the eastern tropical South Pacific oxygen deficient zone. Deep Sea Res. Part I Oceanogr. Res. Pap. 57, 1092–1101. http://dx.doi.org/10.1016/j.dsr.2010.05.009.
- Chang, B.X., Rich, J.R., Jayakumar, A., Naik, H., Pratihary, A.K., Keil, R.G., Ward, B.B., Devol, A.H., 2014. The effect of organic carbon on fixed nitrogen loss in the eastern tropical South Pacific and Arabian Sea oxygen deficient zones. Limnol. Oceanogr. 59, 1267–1274. http://dx.doi.org/10.4319/lo.2014.59.4.1267.
- Chronopoulou, P.-M., Shelley, F., Pritchard, W.J., Maanoja, S.T., Trimmer, M., 2017. Origin and fate of methane in the Eastern Tropical North Pacific oxygen minimum zone. ISME J. 11, 1386–1399. http://dx.doi.org/10.1038/ismej.2017.6.
- Cline, J.D., Kaplan, I.R., 1975. Isotopic fractionation of dissolved nitrate during denitrification in the eastern tropical north pacific ocean. Mar. Chem. 3, 271–299.
- Dähnke, K., Thamdrup, B., 2013. Nitrogen isotope dynamics and fractionation during sedimentary denitrification in Boknis Eck, Baltic Sea. Biogeosciences 10, 3079–3088. http://dx.doi.org/10.5194/bg-10-3079-2013.
- De Brabandere, L., Canfield, D.E., Dalsgaard, T., Friederich, G.E., Revsbech, N.P., Ulloa, O., Thamdrup, B., 2014. Vertical partitioning of nitrogen-loss processes across the oxic-anoxic interface of an oceanic oxygen minimum zone. Environ. Microbiol. 16, 3041–3054. http://dx.doi.org/10.1111/1462-2920.12255.
- Deutsch, C., Brix, H., Ito, T., Frenzel, H., Thompson, L., 2011. Climate-forced variability of ocean hypoxia. Science 333, 336–339. http://dx.doi.org/10.1126/science. 1202422.
- DeVries, T., Deutsch, C., Primeau, F., Chang, B., Devol, A., 2012. Global rates of water-column denitrification derived from nitrogen gas measurements. Nat. Geosci. 5, 547–550. http://dx.doi.org/10.1038/ngeo1515.
- DeVries, T., Deutsch, C., Rafter, P.A., Primeau, F., 2013. Marine denitrification rates determined from a global 3-D inverse model. Biogeosciences 10, 2481–2496. http:// dx.doi.org/10.5194/bg-10-2481-2013.
- Emerson, S., Stump, C., Wilbur, D., Quay, P., 1999. Accurate measurement of O<sub>2</sub>, N<sub>2</sub>, and Ar gases in water and the solubility of N<sub>2</sub>. Mar. Chem. 64, 337–347. http://dx.doi. org/10.1016/S0304-4203(98)00090-5.
- Fiedler, P.C., Talley, L.D., 2006. Hydrography of the eastern tropical Pacific: a review. Prog. Oceanogr. 69, 143–180. http://dx.doi.org/10.1016/j.pocean.2006.03.008.
- Fuchsman, C.A., Devol, A.H., Saunders, J.K., McKay, C., Rocap, G., 2017. Niche Partitioning of the N cycling microbial community of an offshore Oxygen Deficient Zone, Front. Microbiol. 8, 2384.
- Fuchsman, C.A., Murray, J.W., Konovalov, S.K., 2008. Concentration and natural stable isotope profiles of nitrogen species in the Black Sea. Mar. Chem. 111, 90–105. http:// dx.doi.org/10.1016/j.marchem.2008.04.009.
- Ganesh, S., Bristow, L.A., Larsen, M., Sarode, N., Thamdrup, B., Stewart, F.J., 2015. Size-fraction partitioning of community gene transcription and nitrogen metabolism in a marine oxygen minimum zone. ISME J. 9, 2682–2696. http://dx.doi.org/10.1038/ismei.2015.44.
- Ganesh, S., Parris, D.J., DeLong, E.F., Stewart, F.J., 2014. Metagenomic analysis of size-fractionated picoplankton in a marine oxygen minimum zone. ISME J. 8, 187–211. http://dx.doi.org/10.1038/ismej.2013.144.
- Garcia-Robledo, E., Padilla, C.C., Aldunate, M., Stewart, F.J., Ulloa, O., Paulmier, A., Gregori, G., Revsbech, N.P., 2017. Cryptic oxygen cycling in anoxic marine zones. Proc. Natl. Acad. Sci. USA 114, 8319–8324. http://dx.doi.org/10.1073/pnas. 1619844114.
- Garcia, H.E., Locarnini, R.A., Boyer, T.P., Antonov, J.I., Mishonov, A.V., Baranova, O.K., Zweng, M.M., Reagan, J.R., Johnson, D.R., 2013. World Ocean Atlas 2013. Vol. 3: Dissolved Oxygen, Apparent Oxygen Utilization, and Oxygen Saturation. S. Levitus, Ed.; A. Mishonov, Technical Ed. 3, 27.
- Gaye, B., Nagel, B., Dähnke, K., Rixen, T., Emeis, K.C., 2013. Evidence of parallel denitrification and nitrite oxidation in the ODZ of the Arabian Sea from paired stable isotopes of nitrate and nitrite. Glob. Biogeochem. Cycles 27, 1059–1071. http://dx.doi.org/10.1002/2011GB004115.
- Granger, J., Sigman, D.M., 2009. Removal of nitrite with sulfamic acid for nitrate N and O isotope analysis with the denitrifier method. Rapid Commun. Mass Spectrom. 23, 3753–3762.
- Granger, J., Sigman, D.M., Lehmann, M.F., Tortell, P.D., 2008. Nitrogen and oxygen isotope fractionation during dissimilatory nitrate reduction by denitrifying bacteria. Limnol. Oceanogr. 53, 2533–2545. http://dx.doi.org/10.4319/lo.2008.53.6.2533.
- Granger, J., Vt, C., Sigman, D.M., Needoba, J.A., Harrison, P.J., 2004. Coupled nitrogen and oxygen isotope fractionation of nitrate during assimilation by cultures of marine phytoplankton. Limnol. Oceanogr. 49, 1763–1773.
- Großkopf, T., Mohr, W., Baustian, T., Schunck, H., Gill, D., Kuypers, M.M.M., Lavik, G., Schmitz, R.A., Wallace, D.W.R., Laroche, J., 2012. Doubling of marine dinitrogen-fixation rates based on direct measurements. Nature 488, 361–364. http://dx.doi.org/10.1038/nature11338.
- Hamme, R.C., Emerson, S.R., 2004. The solubility of neon, nitrogen and argon in distilled water and seawater. Deep Sea Res. Part I Oceanogr. Res. Pap. 51, 1517–1528. http://dx.doi.org/10.1016/j.dsr.2004.06.009.
- Horak, R.E.A., Ruef, W., Ward, B.B., Devol, A.H., 2016. Expansion of denitrification and anoxia in the eastern tropical North Pacific from 1972 to 2012. Geophys. Res. Lett. 43, 5252–5260. http://dx.doi.org/10.1002/2016GL068871.
- Hu, H., Bourbonnais, A., Larkum, J., Bange, H.W., Altabet, M.A., 2016. Nitrogen cycling in shallow low-oxygen coastal waters off Peru from nitrite and nitrate nitrogen and oxygen isotopes. Biogeosciences 13, 1453–1468. http://dx.doi.org/10.5194/bg-13-1453-2016.

- Ito, T., Deutsch, C., 2013. Variability of the oxygen minimum zone in the tropical North Pacific during the late twentieth century. Glob. Biogeochem. Cycles 27, 1119–1128. http://dx.doi.org/10.1002/2013GB004567.
- Ito, T., Deutsch, C., 2006. Understanding the saturation state of argon in the thermocline: the role of air-sea gas exchange and diapycnal mixing. Glob. Biogeochem. Cycles 20, 1–15
- Ito, T., Minobe, S., Long, M.C., Deutsch, C., 2017. Upper ocean O<sub>2</sub> trends: 1958–2015. Geophys. Res. Lett. 44, 4214–4223. http://dx.doi.org/10.1002/2017GL073613.
- Ito, T., Nenes, A., Johnson, M.S., Meskhidze, N., Deutsch, C., 2016. Acceleration of oxygen decline in the tropical Pacific over the past decades by aerosol pollutants. Nat. Geosci. 9, 443–448. http://dx.doi.org/10.1038/NGEO2717.
- Jayakumar, A., Chang, B.X., Widner, B., Bernhardt, P., Mulholland, M.R., Ward, B.B., 2017. Biological nitrogen fixation in the oxygen-minimum region of the eastern tropical North Pacific ocean. ISME J. 11, 2356–2367. http://dx.doi.org/10.1038/ ismei.2017.97.
- Jayakumar, D.A., Naqvi, S.W.A., Narvekar, P.V., George, M.D., 2001. Methane in coastal and offshore waters of the Arabian Sea. Mar. Chem. 74, 1–13. http://dx.doi.org/10. 1016/S0304-4203(00)00089-X.
- Jensen, M.M., Petersen, J., Dalsgaard, T., Thamdrup, B., 2009. Pathways, rates, and regulation of N<sub>2</sub> production in the chemocline of an anoxic basin, Mariager Fjord, Denmark. Mar. Chem. 113, 102–113. http://dx.doi.org/10.1016/j.marchem.2009. 01.002
- Keil, R.G., Neibauer, J.A., Biladeau, C., Van Der Elst, K., Devol, A.H., 2016. A multiproxy approach to understanding the "enhanced" flux of organic matter through the oxygen-deficient waters of the Arabian Sea. Biogeosciences 13, 2077–2092. http://dx.doi.org/10.5194/bg-13-2077-2016.
- Knox, M., Quay, P.D., Wilbur, D.O., 1992. Kinetic isotopic fractionation during air-water gas transfer of O<sub>2</sub>, N<sub>2</sub>, CH<sub>4</sub>, and H<sub>2</sub>. J. Geophys. Res. 97, 335–343. http://dx.doi.org/ 10.1029/92JC00949.
- Konno, U., Tsunogai, U., Komatsu, D.D., Daita, S., Nakagawa, F., Tsuda, A., Matsui, T., Eum, Y.-J., Suzuki, K., 2010. Determination of total N<sub>2</sub> fixation rates in the ocean taking into account both the particulate and filtrate fractions. Biogeosciences 7, 2369–2377. http://dx.doi.org/10.5194/bg-7-2369-2010.
- Kritee, K., Sigman, D.M., Granger, J., Ward, B.B., Jayakumar, A., Deutsch, C., 2012. Reduced isotope fractionation by denitrification under conditions relevant to the ocean. Geochim. Cosmochim. Acta 92, 243–259. http://dx.doi.org/10.1016/j.gca. 2012.05.020.
- Lehmann, M.F., Sigman, D.M., Mccorkle, D.C., Granger, J., Hoffmann, S., Cane, G., Brunelle, B.G., 2007. The distribution of nitrate 15N/14N in marine sediments and the impact of benthic nitrogen loss on the isotopic composition of oceanic nitrate. Geochim. Cosmochim. Acta 71, 5384–5404. http://dx.doi.org/10.1016/j.gca.2007. 07.025.
- Macko, S.A., Engel, M.H., Qian, Y., 1994. Early diagenesis and organic matter preservation a molecular stable carbon isotope perspective. Chem. Geol. 114, 365–379. http://dx.doi.org/10.1016/0009-2541(94)90064-7.
- Manning, C.C., Hamme, R.C., Bourbonnais, A., 2010. Impact of deep-water renewal events on fixed nitrogen loss from seasonally-anoxic Saanich Inlet. Mar. Chem. 122, 1–10. http://dx.doi.org/10.1016/j.marchem.2010.08.002.
- Marconi, D., Kopf, S., Rafter, P.A., Sigman, D.M., 2017. Aerobic respiration along isopycnals leads to overestimation of the isotope effect of denitrification in the ocean water column. Geochim. Cosmochim. Acta 197, 417–432. http://dx.doi.org/10.1016/j.gca.2016.10.012.
- Mariotti, A., Germon, J.C., Hubert, P., Kaiser, P., Letolle, R., Tardieux, A., Tardieux, P., 1981. Experimental determination of nitrogen kinetic isotope fractionation-some principles– illustration for the denitrification and nitrification processes. Plant Soil 62, 413–430
- Martin, T.S., Casciotti, K.L., 2017. Paired N and O isotopic analysis of nitrate and nitrite in the Arabian Sea oxygen deficient zone. Deep. Res. Part I Oceanogr. Res. Pap. 121, 121–131. http://dx.doi.org/10.1016/j.dsr.2017.01.002.
- Martin, T.S., Casciotti, K.L., 2016. Nitrogen and oxygen isotopic fractionation during microbial nitrite reduction. Limnol. Oceanogr. 61, 1134–1143. http://dx.doi.org/10. 1002/lno.10278.
- McIlvin, M.R., Altabet, M.A., 2005. Chemical conversion of nitrate and nitrite to nitrous oxide for nitrogen and oxygen isotopic analysis in freshwater and seawater. Anal. Chem. 77, 5589–5595. http://dx.doi.org/10.1021/ac050528s.
- McIlvin, M.R., Casciotti, K.L., 2011. Technical updates to bacterial method for nitrate isotopic analyses. Anal. Chem. 83, 1850–1856.
- Mohr, W., Grosskopf, T., Wallace, D.W.R., LaRoche, J., 2010. Methodological underestimation of oceanic nitrogen fixation rates. PLoS One 5, e12583. http://dx.doi.org/ 10.1371/journal.pone.0012583.
- Moisander, P.H., Beinart, R.A., Hewson, I., White, A.E., Johnson, K.S., Carlson, C.A., Montoya, J.P., Zehr, J.P., 2010. Unicellular cyanobacterial distributions broaden the oceanic N<sub>2</sub> fixation domain. Science 327, 1512–1514. http://dx.doi.org/10.1126/ science.1185468.

- Moore, C.M., Mills, M.M., Arrigo, K.R., Berman-Frank, I., Bopp, L., Boyd, P.W., Galbraith, E.D., Geider, R.J., Guieu, C., Jaccard, S.L., Jickells, T.D., La Roche, J., Lenton, T.M., Mahowald, N.M., Marañón, E., Marinov, I., Moore, J.K., Nakatsuka, T., Oschlies, A., Saito, M.A., Thingstad, T.F., Tsuda, A., Ulloa, O., 2013. Processes and patterns of oceanic nutrient limitation. Nat. Geosci. 6, 701–710. http://dx.doi.org/10.1038/pseq1765.
- Paulmier, A., Ruiz-Pino, D., 2009. Oxygen minimum zones (OMZs) in the modern ocean.

  Prog. Oceanogr. 80, 113–128. http://dx.doi.org/10.1016/j.pocean.2008.08.001.
- Peng, X., Fuchsman, C.A., Jayakumar, A., Oleynik, S., Martens-Habbena, W., 2015. Ammonia and nitrite oxidation in the Eastern Tropical North Pacific. Glob. Biogeochem. Cycles 29, 2034–2049.
- Penn, J., Weber, T., Deutsch, C., 2016. Microbial functional diversity alters the structure and sensitivity of oxygen deficient zones. Geophys. Res. Lett. 43, 9773–9780. http:// dx.doi.org/10.1002/2016GL070438.
- Pennington, J.T., Mahoney, K.L., Kuwahara, V.S., Kolber, D.D., Calienes, R., Chavez, F.P., 2006. Primary production in the eastern tropical Pacific: a review. Prog. Oceanogr. 69, 285–317. http://dx.doi.org/10.1016/j.pocean.2006.03.012.
- Peters B., Casciotti K. L., Horak R., Devol, A.H., Fuchsman, C.A., Forbes, M., Mordy, C. (in revision) Estimated fixed nitrogen loss and associated isotope effects using concentrations and isotopic measurements of NO<sub>3</sub>-, NO<sub>2</sub>-, and N<sub>2</sub> from the Eastern Tropical South Pacific oxygen deficient zone. Deep Sea Research II.
- Peters, B.D., Babbin, A.R., Lettmann, K.A., Mordy, C.W., Ulloa, O., Ward, B.B., Casciotti, K.L., 2016. Vertical modeling of the nitrogen cycle in the eastern tropical South Pacific oxygen deficient zone using high-resolution concentration and isotope measurements (GB005415). Glob. Biogeochem. Cycles 30. http://dx.doi.org/10.1002/2016GB005415. Received.
- Rafter, P.A., Difiore, P.J., Sigman, D.M., 2013. Coupled nitrate nitrogen and oxygen isotopes and organic matter remineralization in the Southern and Pacific Oceans. J. Geophys. Res. Ocean. 118, 4781–4794. http://dx.doi.org/10.1002/jgrc.20316.
- Reeburgh, W.S., Ward, B.B., Whalen, S.C., Sandbeck, K.A., Kilpatrickt, K.A., Kerkhof, L.J., 1991. Black Sea methane geochemistry. Deep Sea Res. Part A Oceanogr. Res. Pap. 38, S1189–S1210. http://dx.doi.org/10.1016/S0198-0149(10)80030-5.
- Revsbech, N.P., Larsen, L.H., Gundersen, J., Dalsgaard, T., Ulloa, O., Thamdrup, B., 2009.

  Determination of ultra-low oxygen concentrations in oxygen minimum zones by the STOX sensor. Limnol. Oceanogr. 7, 371–381.
- Saino, T., Hattori, A., 1980. 15N natural abundance in oceanic suspended particulate matter. Nature 283, 752–754. http://dx.doi.org/10.1038/283752a0.
- Sigman, D.M., Casciotti, K.L., Andreani, M., Barford, C., Galanter, M., Böhlke, J.K., 2001.
  A bacterial method for the nitrogen isotopic analysis of nitrate in seawater and freshwater. Anal. Chem. 73, 4145–4153. http://dx.doi.org/10.1021/ac010088e.
- Sigman, D.M., Difiore, P.J., Hain, M.P., Deutsch, C., Karl, D.M., Bo, V., 2009. Sinking organic matter spreads the nitrogen isotope signal of pelagic denitrification in the North Pacific. Geophys. Res. Lett. 36, 1–5. http://dx.doi.org/10.1029/ 2008GI.035784.
- Sigman, D.M., Robinson, R., Knapp, A.N., Geen, A. Van, Mccorkle, D.C., Brandes, J.A., Thunell, R.C., 2003. Distinguishing between water column and sedimentary denitrification in the Santa Barbara Basin using the stable isotopes of nitrate. Geochem. Geophys. Geosystems 4, 1040. http://dx.doi.org/10.1029/2002GC000384.
- Smith, W.H., Sandwell, D., 1997. Global sea floor topography from satellite altimetry and ship depth soundings. Science 277, 1956–1962. http://dx.doi.org/10.1126/science. 277.5334.1956.
- Stramma, L., Johnson, G.C., Sprintall, J., Mohrholz, V., 2008. Expanding oxygenminimum zones in the tropical oceans. Science 320, 655–658.
- Ulloa, O., Delong, E.F., Letelier, R.M., Stewart, F.J., 2012. Microbial oceanography of anoxic oxygen minimum zones. Proc. Natl. Acad. Sci. USA 109, 15996–16003. http:// dx.doi.org/10.1073/pnas.1205009109.
- UNESCO, 1994. Protocols for the Joint Global Ocean Flux Study (JGOFS) Core Measurements. New York.
- Voss, M., Dippner, J.W., Montoya, J.P., 2001. Nitrogen isotope patterns in the oxygendeficient waters of the Eastern Tropical North Pacific Ocean. Deep Sea Res. Part I Oceanogr. Res. Pap. 48, 1905–1921.
- Wada, E., 1980. Nitrogen isotope fractionation in biogeochemical processes occurring in marine environments. In: Goldberg, E.D., Horibe, Y. (Eds.), Isotope Marine Chemistry. Uchida Rokakuho, Tokyo, pp. 375–398.
- Ward, B.B., Devol, A.H., Rich, J.J., Chang, B.X., Bulow, S.E., Naik, H., Pratihary, A.K., Jayakumar, A., 2009. Denitrification as the dominant nitrogen loss process in the Arabian Sea. Nature 461, 78.
- Whitney, F.A., Freeland, H.J., Robert, M., 2007. Persistently declining oxygen levels in the interior waters of the eastern subarctic Pacific. Prog. Oceanogr. 75, 179–199. http://dx.doi.org/10.1016/j.pocean.2007.08.007.
- Wilson, S.T., del Valle, D.A., Segura-Noguera, M., Karl, D.M., 2014. A role for nitrite in the production of nitrous oxide in the lower euphotic zone of the oligotrophic North Pacific Ocean. Deep. Res. Part I Oceanogr. Res. Pap. 114, 47–55. http://dx.doi.org/ 10.1016/j.dsr.2013.11.008.